X-ray Flashes from Off-axis Nonuniform Jets *

Zhi-Ping Jin and Da-Ming Wei

Purple Mountain Observatory, Chinese Academy of Sciences, Nanjing 210008; jin@pmo.ac.cn
National Astronomical Observatories, Chinese Academy of Sciences, Beijing 100012

Abstract   It has been widely believed that the outflows in gamma-ray bursts are
jetted and some jets may have structures like $\epsilon(\theta) \propto \theta^{-k}$. We check the possibility
that X-ray flashes come from such jets. Both qualitative and quantitative analyses
have shown that this model can reproduce most of the observational features of both
X-ray flashes and gamma-ray bursts. Using the usual parameters of gamma-ray
bursts, we have carried out numerical calculations for both uniform and nonuniform
jets, of their fluxes, spectra and peak energies. It seems that nonuniform jets are
more appropriate to these observational properties than uniform jets. We have
also shown that in our model the observational ratio of gamma-ray bursts to X-ray
flashes is about a few units.

Key words: X-rays: general — gamma rays: bursts — ISM: jets and outflows

1   INTRODUCTION

X-ray flash (XRF) is one of the more recently identified types of explosion. It is qualitatively
similar to the gamma-ray burst (GRB) in most of its properties such as duration, temporal
structure, spectrum and spectral evolution, but not as regarding the peak energy and flux. The
peak energy and flux of the XRF are lower, its spectral distribution joins smoothly to that
of the GRB. There seems to be no obvious borderline between the XRF and the GRB. These
similarities have led to the suggestion that the X-ray flash is in fact "X-ray rich" gamma-ray
burst (Kippen et al. 2003). It is likely they have the same origin but different conditions of
generation.

The similarity between XRF and GRB suggests that an XRF might come from an off-axis
nonuniform jet of a GRB (Woosley et al. 2003; Rossi et al. 2002a; Zhang & Mészáros 2002b).
When a burst is observed at the center of the jet, it will be detected as a normal gamma-ray
burst, but when it is observed at a large viewing angle, it tends to be "dirty" (Zhang & Mészáros
2002b), for matter ejected off-axis takes less energy and has a lower Lorentz factor, the peak
energy E_{p} shifts to the X-ray frequencies, and then the burst is observed as an X-ray flash.

In this paper, we adopt a structured jet model in which the energy and both the mass of

---

ejected matter per unit solid angle and the initial bulk Lorentz factor depend on the angular distance from the center, θ, according to a power law: $\epsilon(\theta) \propto (\theta/\theta_c)^{-k}$, $m_{ej}(\theta) \propto (\theta/\theta_c)^{-k_2}$, and $\gamma(\theta) \propto (\theta/\theta_c)^{-k_1}$ (Mészáros et al. 1998; Rossi et al. 2002b). Rossi et al. (2002a) have shown that $1.5 \leq k \leq 2.2$ gives a reasonably good fit to the observations. We take $k = 2$ for our calculations.

Frail et al. (2001) have considered the distribution of jet angles for GRBs of known redshifts. The opening angle ranges from 0.05 to 0.4 rad, and the most common value is 0.12 rad (Perna et al. 2003). The gamma-ray energies released are narrowly clustered around $E_\gamma \sim 5 \times 10^{50}$ erg.

In Sect. 2, we introduce our model and present some analytical solutions. In Sect. 3 we present our numerical results of the spectra and fluxes for both uniform and nonuniform jets, and our calculation of the observed GRB to XRF ratio. In Sect. 4, we give a discussion and draw some conclusions.

2   THE MODEL

We consider a relativistic outflow for which the energy per unit solid angle has a power-law dependence on the angular distance θ from the center (Mészáros et al. 1998; Zhang & Mészáros 2002a; Rossi et al. 2002a):

$$\epsilon(\theta) = \begin{cases} \epsilon_c & 0 \leq \theta \leq \theta_c \\ \epsilon_c(\frac{\theta}{\theta_c})^{-k} & \theta_c \leq \theta \leq \theta_j \\ 0 & \theta_j \leq \theta \end{cases}, \tag{1}$$

and the ejected mass per unit solid angle and the bulk Lorentz factor also depend on θ according to power laws: $m_{ej}(\theta) = m_{ej}(0)(\theta/\theta_c)^{-k_2}$, $\gamma(\theta) = \gamma(0)(\theta/\theta_c)^{-k_1}$ ($\theta_c \leq \theta \leq \theta_j$). The deceleration radius at θ is $r_d(\theta) = (\frac{3\epsilon(\theta)}{4\pi n\gamma(\theta)^2 m_p c^2})^{1/3} = r_d(0)(\frac{\theta}{\theta_c})^{(-k+2k_1)/3}$.

All our calculations will be done for the time when the outflow just reaches its deceleration radius r_d where the blast wave is formed. Because of the beaming effect of the large Lorentz factor at this time, there is no obvious observable difference between isotropic and anisotropic outflows. That means a jetted outflow with a viewing angle θ_v is observationally similar to an isotropic outflow with bulk Lorentz factor $\gamma = \gamma(\theta_v)$. So we can use the solutions from the isotropic explosion model (Sari & Piran 1999) to carry out the analysis by choosing different Lorentz factors at different viewing angles θ_v. The characteristic synchrotron frequency ν_m and the cooling frequency ν_c are:

$$\nu_m(\theta_v) = 44 \, \text{keV} \left(\frac{\epsilon_e}{0.1}\right)^2 \left(\frac{\epsilon_B}{0.1}\right)^{1/2} \left(\frac{\gamma(\theta_v)}{300}\right)^4 n_1^{1/2}, \tag{2}$$

$$\nu_c(\theta_v) = 0.44 \, \text{keV} \left(\frac{\epsilon_B}{0.1}\right)^{-3/2} \left(\frac{\gamma(\theta_v)}{300}\right)^{-4} n_1^{-3/2} t_s^{-2}. \tag{3}$$

The fluxes at ν_c and ν_m are:

$$F_{\nu c}(\theta_v) = 220 \, \mu\text{Jy} \, D_{28}^{-2} \left(\frac{\epsilon_B}{0.1}\right)^{1/2} \left(\frac{\gamma(\theta_v)}{300}\right)^2 \left(\frac{r_d(\theta_v)}{5.4 \times 10^{15}}\right)^3 n_1^{3/2}, \tag{4}$$

$$F_{\nu m}(\theta_v) = F_{\nu c}\left(\frac{\nu_m}{\nu_c}\right)^{-1/2} = 22\mu\text{Jy} \, D_{28}^{-2} \left(\frac{\epsilon_e}{0.1}\right)^{-1} \left(\frac{\epsilon_B}{0.1}\right)^{-1/2} \left(\frac{r_d(\theta_v)}{5.4 \times 10^{15}}\right)^2 n_1^{1/2}, \tag{5}$$

$$\begin{aligned} (\nu F_\nu)_{\max}(\theta_v) &= \nu_m(\theta_v) F_{\nu m}(\theta_v) \\ &= 2.4 \times 10^{-10} \text{erg} \cdot \text{cm}^{-2} \cdot \text{s}^{-1} D_{28}^{-2} \left(\frac{\epsilon_e}{0.1}\right)^1 \left(\frac{\gamma(\theta_v)}{300}\right)^4 \left(\frac{r_d(\theta_v)}{5.4 \times 10^{15}}\right)^2 n_1^1. \end{aligned} \tag{6}$$

Here, ϵ_e, ϵ_B are the fractions of electron and magnetic energy density, $D_{28} = D/10^{28}$cm is the distance of the source, $n_1 = n/1$cm^{-3} is the particle density of external medium and $t_s = t/1$s is the observer time. These equations describe the emission features from a blast wave. Generally, an external shock is not ideal for reproducing a highly variable burst (Sari et al. 1998), but it can reproduce a burst with several peaks (Panaitescu & Mészáros 1998) and therefore may be applicable to the class of long, smooth bursts (Mészáros 1999).

Electrons in the external medium will be accelerated to a power law distribution. These electrons will produce a broken power law spectrum with photon spectrum indexes α (low) and β (high) in the range $-3/2$ to $-2/3$ and $-(p+1)/2$ to $-(p+2)/2$ through synchrotron emission (Katz 1994; Cohen et al. 1997; Lloyd & Petrosian 2000). Here p is the power law index of the accelerated electrons. When an anisotropic burst is viewed from different directions, E_p may change from several keV (or several eV, depending on $\gamma(0)$, θ_j, θ_c and k) to hundreds keV (or several MeV). This remark applies to both GRBs and XRFs.

From Eqs.(2) and (6), we obtain:

$$\nu_m(\theta) \propto \gamma^4(\theta) \propto \gamma^4(0)\left(\frac{\theta}{\theta_c}\right)^{-4k_1}, \tag{7}$$

$$(\nu F_\nu)_{max}(\theta) \propto \gamma^4(\theta)r_d^2(\theta) \propto \gamma^4(0)r_d^2(0)\left(\frac{\theta}{\theta_c}\right)^{-\frac{2}{3}k-\frac{8}{3}k_1}. \tag{8}$$

Comparing Eqs. (7) and (8) we obtain:

$$F(\theta) \sim (\nu F_\nu)_{max}(\theta) \propto \nu_m^\delta(\theta). \tag{9}$$

Here, $\delta = \frac{k+4k_1}{6k_1}$ only depends on the relation between k and k_1. If we assume simply $k_1 = k_2 = k/2$ and a constant $\gamma(0)$ for every explosion, then we will obtain $\delta = 1$ which will lead to the conclusion $E_p \propto L$. In order to obtain the observational relation $E_p \propto L^{1/2}$ (Lloyd et al. 2000; Amati et al. 2002; Wei & Gao 2003), we will assume $k_1 \sim \frac{1}{8}k$.

Yamazaki et al. (2002) have suggested that X-ray flashes come from isotropic jets when $\theta_v > \theta_j$, and have $F_{\nu m} \propto (\gamma(1 - \beta\cos(\theta_v - \theta_j)))^{-3}$. In this case, $\nu_m \propto (\gamma(1 - \beta\cos(\theta_v - \theta_j)))^{-1}$ (Granot et al. 2002), we then find that δ is about 4 and $E_p \propto L^{1/4}$.

Outflows with a lower Lorentz factor, called a "dirty" fireball or a failed gamma-ray burst, may also produce a X-ray flash (Heise et al. 2003; Huang et al. 2002), with a similar spectrum and flux to those we gave above for a nonuniform jet. This means that we cannot distinguish our model from a dirty fireball model just by a single X-ray flash. By simply assuming the bulk Lorentz factor $\Gamma \propto L^{1/4\delta}$, we can obtain $E_p \propto \Gamma^4 \propto L^{1/\delta}$. This means maybe we cannot distinguish nonuniform jet model from the dirty fireball model even by statistical properties.

3 NUMERICAL RESULT

We have derived some useful conclusions using a simplified analysis. More realistically, the observed flux at frequency ν is an integral over the equal arrival time surface of the jet:

$$F_\nu = \int_{\gamma_{min}}^{\gamma_{max}} d\gamma_e \int_0^{2\pi} d\phi \int_0^{\theta_j} \sin\theta d\theta D^3 \frac{P'(\nu D^{-1})N(\gamma_e)}{4\pi d_L^2}. \tag{10}$$

Here $P'(\nu') = \frac{\sqrt{3}e^3 B}{m_e c}f(\chi)$ is synchrotron radiation power at frequency ν' from a single electron in the fireball co-moving frame (Rybicki & Lightman 1979), $D = (\gamma(\theta)(1 - \beta\cos\Theta))^{-1}$ is the

Doppler factor translating from the fireball co-moving frame to the observer's frame, Θ is the angle between the direction the outflow and the line-of-sight. The electron number distribution can be written as (Dai et al. 1999):

1. For $\gamma_c \leq \gamma_{e,mim}$

$$N(\gamma_e) = \begin{cases} C_1 \gamma_e^{-2} & \gamma_c \leq \gamma_e \leq \gamma_{e,min} \\ C_2 \gamma_e^{-(p+1)} & \gamma_{e,min} \leq \gamma_e \leq \gamma_{e,max} \end{cases}, \tag{11}$$

where

$$C_1 = C_2 \gamma_{min}^{-p+1},$$

$$C_2 = \left[\frac{\gamma_{e,min}^{1-p} - \gamma_c^{1-p}}{\gamma_c(p-1)} + \frac{\gamma_c^{-p} - \gamma_{e,max}^{-p}}{p} \right]^{-1} N_e,$$

$N_e = \frac{1}{3} r^3 n_1$ is the total number of electrons per unit solid angle and is equal to the number of protons in the swept ISM, γ_c is the critical electron Lorentz factor above which the synchrotron radiation is significant (Sari et al. 1998),

$$\gamma_c = \frac{3m_e}{16\epsilon_B \sigma_T m_p c} \times \frac{1}{t\gamma^3 n} = \frac{3m_e}{8\sigma_T m_p} \epsilon_B^{-1} \gamma(\theta)^{-1} r(\theta)^{-1} n_1^{-1}. \tag{12}$$

2. For $\gamma_{e,min} \leq \gamma_c \leq \gamma_{e,max}$

$$N(\gamma_e) = \begin{cases} C_3 \gamma_e^{-p} & \gamma_{e,min} \leq \gamma_e \leq \gamma_c \\ C_4 \gamma_e^{-(p+1)} & \gamma_c \leq \gamma_e \leq \gamma_{e,max} \end{cases}, \tag{13}$$

where $C_3 = C_4 \gamma_{min}^{-p+1}$, $C_4 = [\gamma_c^{-1} \gamma_{e,min}^{1-p} + \frac{(1-p)\gamma_{e,min}^{-p} - \gamma_{e,max}^{-p}}{p}]^{-1} N_e$.

3. For $\gamma_c \geq \gamma_{e,max}$

$$N(\gamma_e) = C_5 \gamma_e^{-p} \quad \gamma_{e,min} \leq \gamma_e \leq \gamma_{e,max}, \tag{14}$$

where $C_5 = \frac{p-1}{\gamma_{e,min}^{1-p} - \gamma_{e,max}^{1-p}} N_e$.

We assume that the bulk Lorentz factor $\gamma(\theta)$ stays a constant before the outflow arrives at the deceleration radius r_d. Here we choose $k_1 = k_2$ which makes r_d a constant at different θ. This assumption will simplify the calculations. However, it should be noted that for different θ the time for the outflow to reach r_d is different. We calculate this arrival time for viewing angle θ_v by:

$$T = \frac{(1 - \beta \cos(\max[\theta_v - \theta_j, 0]))r_d}{\beta c}. \tag{15}$$

The equal arrival time surface at θ is:

$$r(\theta) = \frac{\beta c T}{1 - \beta \cos \Theta}. \tag{16}$$

Our numerical results are shown in Figs.1 and 2. We chose $\theta_j = 0.1$, $\theta_c = 0.02$, $\gamma_0 = 500$, $r_d = 4.0 \times 10^{16}$cm, $d_L = 1 \times 10^{28}$cm, $\epsilon_e = 0.1$, $\epsilon_B = 0.1$, $p = 2.5$ and $k = 2$ for a nonuniform jet and $k = 0$ for a uniform one.

It seems that for a nonuniform jet, the spectra and fluxes fit both the GRB and XRF observations fairly well. Viewed from the center, E_p is about $100\,\mathrm{keV} \sim 1\,\mathrm{MeV}$, and the flux is about $10^{-7} \sim 10^{-6}$ erg cm^{-2}s^{-1}. These are typical values of GRBs (e.g., in Fig.1, the cases for $\theta_v = 0, 0.02, 0.04$). When viewed from off-axis, E_p is about $10 - 100\,\mathrm{keV}$, the flux is about $10^{-8} \sim 10^{-7}$ erg cm^{-2} s^{-1} (e.g., in Fig. 1, the cases for $\theta_v = 0.04, 0.06$). These are typical
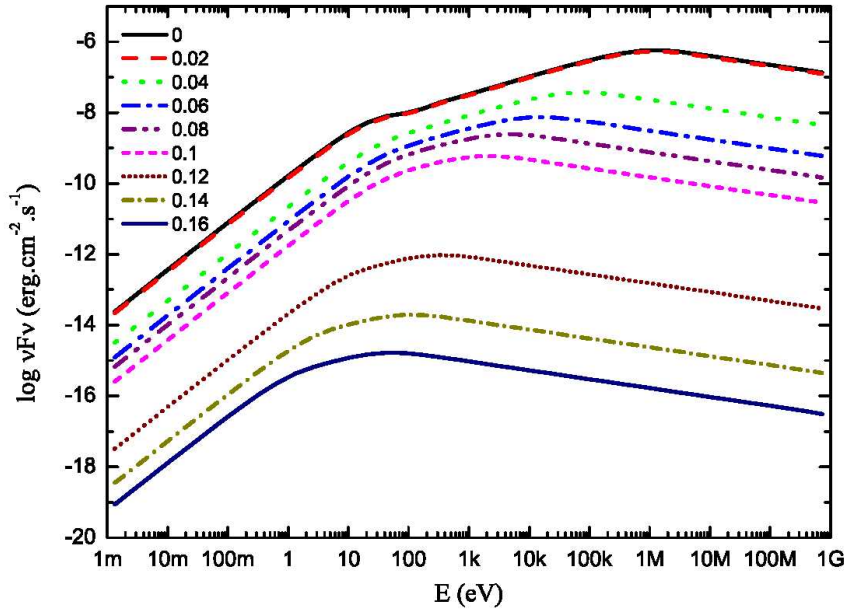
Fig. 1   Spectra of a *non-uniform* jet viewed from different viewing angles between 0 and 0.16, for $\theta_j = 0.1$, $\theta_c = 0.02$, $k = 2$, $k_1 = k_2 = k/2$, $r_d = 4.0 \times 10^{16}$cm, $\gamma(0) = 500$, $p = 2.5$.

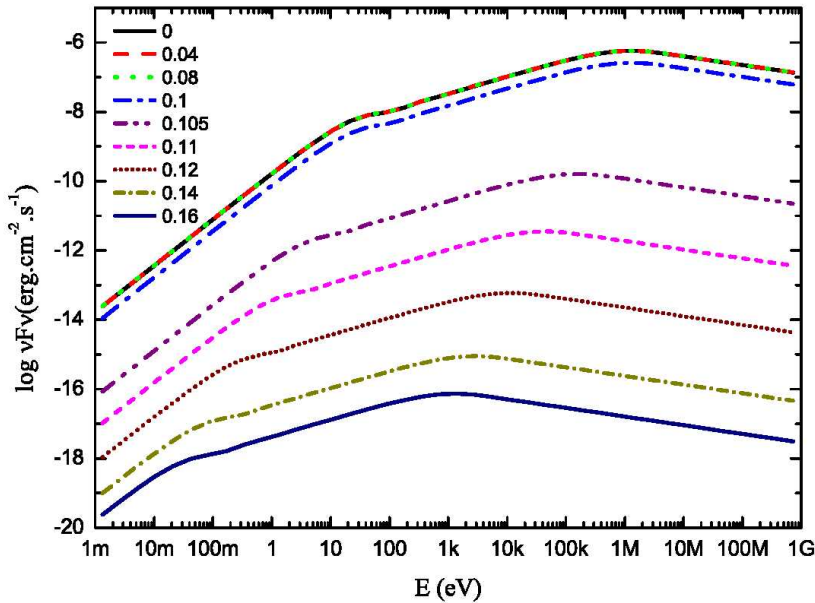Fig. 2   Spectra of a *uniform* jet viewed from different viewing angles between 0 and 0.16, for $\theta_j = 0.1$, $r_d = 4.0 \times 10^{16}$cm, $\gamma = 500$ and $p = 2.5$. The spectra for angles between 0 and 0.08 overlap.

values of XRFs. When $\theta_{\rm v} = 0.08, 0.1$, $E_{\rm p}$ is about a few keV, the flux seems a little low but can still be detected if the distance of the source is not too large.

However, it appears that for a uniform jet, the flux from the edge of the jet (where XRFs are thought to originate in this model) is somewhat too low. In this case the spectral peak is at 10–100 keV, the flux is about $10^{-13} \sim 10^{-10}$ erg cm^{-2} s^{-1} (see, e.g., Fig.2, for the cases $\theta_{\rm v} = 0.105, 0.11, 0.12$). It can only explain nearby XRFs, such as $z \leq 0.2$ (Yamazaki et al. 2002). However, XRFs are more likely to have cosmological origins (Heise 2002). To explain a cosmic X-ray flash with a uniform jet, one must assume an improbably small horn angle (Yamazaki et al. 2003).

We assume that all explosions have the same luminosity and jet shape, with luminosity at center $L_\nu(0)$, then at viewing angle θ we have $L_\nu(\theta) = L_\nu(0)(\theta/\theta_{\rm c})^{-2k_1}$. Depending on the viewing angle θ, a burst can be detected only to a distance:

$$D(\theta) \leq D_{\rm max}(\theta) = \Big(\frac{L_\nu(0)(\theta/\theta_{\rm c})^{-2k_1}}{4\pi F_{\nu,\rm min}}\Big)^{1/2}, \tag{17}$$

where $F_{\nu,\rm min}$ is the threshold of the detector. So the numbers of GRBs ($N_{\rm GRBs}$) and XRFs ($N_{\rm XRFs}$) are:

$$N_{\rm GRBs} = \int_0^{\theta_{\rm c}} \frac{4}{3}\pi D(\theta_{\rm c})^3 n \frac{\sin(\theta)d\theta}{2} + \int_{\theta_{\rm c}}^{\theta_{\rm cr}} \frac{4}{3}\pi D(\theta)^3 n \frac{\sin(\theta)d\theta}{2}, \tag{18}$$

$$N_{\rm XRFs} = \int_{\theta_{\rm cr}}^{\theta_{\rm j}} \frac{4}{3}\pi D(\theta)^3 n \frac{\sin(\theta)d\theta}{2}, \tag{19}$$

where n is the number of bursts per unit volume, $\theta_{\rm cr}$ is the critical angle. If the viewing angle is larger than $\theta_{\rm cr}$ the explosion will be observed as XRFs. We divide XRFs from GRBs with $E_{\rm p} = 90$ keV, and assume the peak energy from the jet axis $E_{\rm p,c} = 1$ MeV, then the critical angle $\theta_{\rm cr} = (\frac{E_{\rm p,c}}{90\,\rm keV})^{\frac{1}{4k_1}}\theta_{\rm c}$. We obtain

$$\frac{N_{\rm GRBs}}{N_{\rm XRFs}} = \frac{\frac{3}{2}\theta_{\rm c}^{-1} - \theta_{\rm cr}^{-1}}{\theta_{\rm cr}^{-1} - \theta_{\rm j}^{-1}} \sim 2.6. \tag{20}$$

We have neglected the cosmic effect in this order of magnitude estimation. This result depends on the parameters we have chosen. Changing these parameters in a reasonable range will change the result a little but not much. On the other hand, these parameters are restricted by the observed ratio.

4 DISCUSSION AND CONCLUSIONS

It is more likely that gamma-ray burst outflows are in the form of jets with nonuniform energy distribution (Dai & Gou 2001; Panaitescu & Kumar 2003). In this paper, we use a structured jet model in which the energy per unit solid angle decreases as $\epsilon(\theta) \propto \theta^{-k}$. We reproduce the key observational features of the XRFs and GRBs. Our calculations are based on the external shock model which does not seem to be ideal for reproducing GRBs with highly variable temporal structure, but appears to be adequate for bursts with smooth light curves. And our calculations can also be adapted to the internal shock model.

We have chosen $\theta_{\rm c} = 0.02$ and $\gamma(0) = 500$ in our numerical calculations. However, the lower limit to $\theta_{\rm c}$ is about $1/\gamma_{\rm max} \sim 10^{-3}$, and the bulk Lorentz factor in the center has a maximum

value to $\gamma_{\mathrm{max}} \sim 10^5$ (Piran 1999; Rossi et al. 2002a). Thus E_{p} may be in excess of MeV when the axis points directly at us though the probability of this happening is small.

We take $k = 2$ for a nonuniform jet. Rossi et al. (2002a) have shown that $1.5 \leq k \leq 2.2$ is a reasonable value for a good fit to the observations (Zhang & Mészáros 2002a). For the range $1 \leq k \leq 3$, the calculated spectra and fluxes as well as the calculated relation between E_{p} and L, are similar to those for $k = 2$. Because of the beaming effect and the shape of the equal arrival time surface, the radiation mainly comes from outflows that point directly towards the observer. We will observe a similar spectrum and flux at a larger (smaller) viewing angle when k is smaller (larger). However, it will change our solution of the GRB to XRF number ratio. We also assumed $k_1 = k_2 = 1$ throughout this paper. If $k_1 \neq k_2$, the calculation would be much more complicated.

We find that the observational GRB to XRF ratio is about a few units in our model. Our model predicts that more XRFs or soft GRBs will be found in the future when more sensitive instruments are launched. Barraud et al. (2003) have presented 35 GRB/XRF spectra from HETE-2 over the range 4–700 keV, of these 35 bursts, 24 have E_{p} higher than 90 keV; 11, lower. The ratio is comparable to our calculated value of ~ 2.6.

Observations have shown a correlation $E_{\mathrm{p}} \propto L^{1/2}$ (Lloyd et al. 2000; Amati et al. 2002; Wei & Gao 2003). This result is still not well explained except for some arguments based on some very simple assumption (Lloyd et al. 2000). We find in our model for a single explosion viewed from different angles, $E_{\mathrm{p}} \propto L^{1/\delta}$. If we simply choose $k_1 = \frac{1}{2}k$, we obtain $\delta = 1$, or we may choose $k_1 = \frac{1}{8}k$ to tally with the observation. For a dirty fireball the relation between the initial Lorentz factor and explosion energy is uncertain. Simply assuming $\Gamma \propto L^{1/8}$ will lead to the same conclusion we have presented.

Our model cannot be distinguished from a dirty fireball model just by a single X-ray flash, but can be so distinguished by such statistical properties as the observational GRB to XRF number ratio. In addition, the two models are different in respect of afterglows. A very obvious feature of the structured jet is that when $\theta_{\mathrm{v}}/\theta_{\mathrm{c}}$ and k is large, there will be a prominent flattening in the afterglow light curve, and a very sharp break occurring at the time $\gamma \sim (\theta_{\mathrm{v}} + \theta_{\mathrm{c}})^{-1}$ after the flattening (Rossi et al. 2002a; Wei & Jin 2003). We suggest that such features are more likely to be found in an X-ray flash afterglow than in a gamma-ray burst afterglow if the XRF does come from an off-axis nonuniform jet, because an XRF has a larger $\theta_{\mathrm{v}}/\theta_{\mathrm{c}}$ value than a GRB has in this model.

Orphan afterglows once caused great expectations to testify to GRB collimation (Rhoads 1997). In a nonuniform jet, orphan afterglows may be generated in two ways. One way is when the viewing angle is outside of the jet edge (e.g. in Fig.1 the cases $\theta_{\mathrm{v}} = 0.12, 0.14, 0.16$, the fluxes will increase to detectable values at later time). In this case, GRBs/XRFs are undetectable due to the beaming effect but afterglows which are less beamed are detectable. The other probable way is that the Lorentz factor along the line of sight is sufficiently small that the peak energy E_{p} is below the X-ray band. This case did not appear in our calculations, and it will appear if we choose a smaller value of $\theta_{\mathrm{c}}/\theta_{\mathrm{j}}$ or a larger value of k_1.

We have neglected the evolution of the bulk Lorentz factor and the lateral expansion of the jet, which would make the calculations more complex and we think these effects are not very important before the outflows arrive at their deceleration radius. Huang et al. (2000) have given in detail the overall evolution of jetted gamma-ray bursts, and we consider all the effects should be into account for more realistic calculations.

References

Amati L., Frontera F., Tavani M. et al., 2002, A&A, 390, 81

Barraud C., Olive J. F., Lestrade J. P. et al., 2003, A&A, 400, 1021

Cohen E., Katz J. I., Piran T. et al., 1997, ApJ, 488, 330

Dai Z. G., Huang Y. F., Lu T., 1999, ApJ, 520, 634

Dai Z. G., Gou L. J., 2001, ApJ, 552, 72

Frail D. A., Kulkarni S. R., Sari R. et al., 2001, ApJ, 562, L55

Granot J., Panaitescu A., Kumar P., Woosley S. E., 2002, ApJ, 570, L61

Heise J., 2002, Talk given in 3rd workshop Gamma-ray Bursts in the afterglow Era

Heise J., in't Zand J. J. M., Kippen R. M., Woods P. M., 2003, AIP Conf. Proc. 662, 229

Huang Y. F., Gou L. J., Dai Z. G., Lu T., 2000, ApJ, 543, 90

Huang Y. F., Dai Z. G., Lu T., 2002, MNRAS, 332, 735

Katz J. I., 1994, ApJ, 432, L107

Kippen R. M., Woods P. M., Heise J. et al., 2003, AIP Conf. Proc. 662, 244

Lloyd N. M., Petrosian V., Mallozzi R. S., 2000, ApJ, 534, 227

Lloyd N. M., Petrosian V., 2000, ApJ, 543, 722

Mészáros P., Rees M. J., Wijers R. A. M. J., 1998, ApJ, 499, 301

Mészáros P., 1999, Cosmic Explosions, Procs. 10th October Astrophysics Conference, Maryland, astro-ph/9912474

Panaitescu A., Mészáros P., 1998, ApJ, 492, 683

Panaitescu A., Kumar P., 2003, ApJ, 592, 390

Perna R., Sari R., Frail D., 2003, ApJ, 594, 379

Rhoads J., 1997, ApJ, 487, L1

Piran T., 1999, Phys. Rep., 314, 575

Rossi E., Lazzati D., Rees M. J., 2002a, MNRAS, 332, 945

Rossi E., Lazzati D., Salmonson J. D., Ghisellini G., 2002b, astro-ph/0211020

Rybicki G. B., Lightman A. P., 1979, Radiative Processes in Astrophysics, New York: Wiley

Sari R., Piran T., Narayan R., 1998, ApJ, 497, L17

Sari R., Piran T., 1999, ApJ, 520, 641

Wei D. M., Gao W. H., 2003, MNRAS, 345, 743

Wei D. M., Jin Z. P., 2003, A&A, 400, 415

Woosley S. E., Zhang W. Q., Heger A., 2003, AIP Conf. Proc., 662, 185

Yamazaki R., Ioka K., Nakamura T., 2002, ApJ, 571, L31

Yamazaki R., Ioka K., Nakamura T., 2003, ApJ, 593, 941

Zhang B., Mészáros P., 2002a, ApJ, 571, 876

Zhang B., Mészáros P., 2002b, ApJ, 581, 1236